

Theoretical Considerations when Estimating the Mesophyll Conductance to CO₂ Flux by Analysis of the Response of Photosynthesis to CO₂¹

Peter C. Harley, Francesco Loreto, Giorgio Di Marco, and Thomas D. Sharkey*

Systems Ecology Research Group, San Diego State University, San Diego, California 92182 (P.C.H.); Istituto di Radiobiochimica ed Ecofisiologia Vegetale, (Consiglio Nazionale delle Ricerche-IREV), Area della Ricerca del CNR, 00016 Monterotondo Scalo, Roma, Italy (F.L., G.D.); and Department of Botany, University of Wisconsin, Madison, Wisconsin 53706 (F.L., T.D.S.)

ABSTRACT

The conductance for CO₂ diffusion in the mesophyll of leaves can limit photosynthesis. We have studied two methods for determining the mesophyll conductance to CO₂ diffusion in leaves. We generated an ideal set of photosynthesis rates over a range of partial pressures of CO₂ in the stroma and studied the effect of altering the mesophyll diffusion conductance on the measured response of photosynthesis to intercellular CO₂ partial pressure. We used the ideal data set to test the sensitivity of the two methods to small errors in the parameters used to determine mesophyll conductance. The two methods were also used to determine mesophyll conductance of several leaves using measured rather than ideal data sets. It is concluded that both methods can be used to determine mesophyll conductance and each method has particular strengths. We believe both methods will prove useful in the future.

The photosynthetic fixation of CO₂ occurs at the enzyme Rubisco that is at the end of a complex diffusion path. The partial pressure of CO₂ drops across any part of the pathway that has a low conductance. Therefore, any low-conductance component of the diffusion path poses a limitation to photosynthesis whenever CO₂ is not saturating. The conductance to diffusion of CO₂ in photosynthesizing leaves is commonly divided into three components: boundary layer, stomatal, and mesophyll conductances (9). Mesophyll conductance has sometimes been defined in such a way that it includes biochemical factors, but we use it here in the more restricted sense of a physical diffusion phenomenon. These conductances may be subdivided further or lumped together in various ways (21), but the simple three-part formulation serves our purpose.

Because CO₂ and water vapor share a common diffusion path from the air to the spaces inside leaves, analysis of water vapor fluxes allows accurate estimates of the boundary layer and stomatal diffusion conductances. These conductances to water vapor can be converted to conductances for CO₂ by dividing the stomatal conductance by 1.6. Both the stomatal and boundary layer conductances to CO₂ will be lumped and called g_s .² A number of studies (17, 20, 27) have confirmed the validity of such estimates of the conductance to CO₂ diffusion through the boundary layer and stomata provided no stomatal heterogeneity occurs (28).

The mesophyll conductance is much more difficult to assess and has often been assumed to be negligibly small (11). However, the plants used to verify models of photosynthesis typically had high rates of photosynthesis that facilitated measurements but probably also selected for plants with high g_m . Indeed, indirect evidence based on stable isotope fractionation and the response of photosynthesis to CO₂ indicated that g_m was large (10). However, this may not hold for plants with thick leaves or with low rates of photosynthesis (22).

Nobel (21) estimated g_m by considering each step of the CO₂ diffusion path (cell wall, plasmalemma, cytosol, chloroplast envelope, and stroma) and estimating the diffusion path length, area available for diffusion, and the diffusion coefficient for each step. This method is not practical for measurements on a large number of plants. Troughton and Slatyer (29) estimated g_m by assuming that departures in the response of photosynthesis to CO₂ from Michaelis-Menten kinetics were caused by g_m .

A low g_m reduces C_c and so methods for estimating C_c can be used to estimate g_m . Three methods for estimating C_c , and from that estimating g_m , have recently been published. The

¹ Research supported by Department of Energy grant FG02-87ER13785 to T.D.S. and National Research Council of Italy, Special Project RAISA, sub-project No. 2, paper No. 252 to G.D. F.L. was supported by Consiglio Nazionale della Ricerche and North Atlantic Treaty Organization fellowships and P.C.H. was supported by a grant from the U.S. Department of Energy CO₂ Research Division No. DE-FG03-86ER60490 to J.F. Reynolds, Systems Ecology Research Group, San Diego State University.

² Abbreviations: g_s , stomatal conductance to CO₂ diffusion (this can be converted to the more often reported conductance to water vapor diffusion by multiplying by 1.6); A, photosynthetic CO₂ assimilation; C_a , ambient CO₂ partial pressure; C_c , partial pressure of CO₂ inside the chloroplast; C_i , partial pressure of CO₂ in the air spaces inside leaves; g_m , mesophyll conductance to CO₂ diffusion; Γ^* , CO₂ compensation point in the absence of R_d ; J, rate of photosynthetic electron transport; R_d , respiration occurring during the day not related to photorespiration; RuBP, ribulose biphosphate; pCO_2 partial pressure of CO₂.

first relies on the fractionation of stable carbon isotopes during photosynthesis. The degree to which the discrimination of Rubisco is expressed during intact leaf photosynthesis depends on the ratio C_c/C_a (8, 18). Because the leaf discriminates against $^{13}\text{CO}_2$, air that passes over a leaf will be enriched in $^{13}\text{CO}_2$. By trapping the CO_2 from an airstream passing over a leaf, Evans *et al.* (6) were able to determine the discrimination expressed by the leaf and, from that, C_c . This technique works well but requires a ratio mass spectrometer as well as a vacuum line adjacent to a gas analysis system for trapping CO_2 . The isotopic method for determining g_m will not be discussed further in this paper; instead we shall focus on two other methods that do not require a ratio mass spectrometer. The methods we shall describe are more likely to find widespread use and may provide a confirmation of the isotopic method (19).

One method, described by Bongi and Loreto (1), exploits the fact that when RuBP regeneration (*i.e.* J) limits photosynthesis, photosynthesis continues to increase with increasing C_i because of the suppression of photorespiration. The response of photosynthesis to CO_2 under these conditions depends upon C_c and the specificity of Rubisco for CO_2 relative to O_2 . The specificity of Rubisco in C_3 plants can be measured *in vitro* (15, 16, 31, 32) and can be estimated by gas-exchange analysis (2). By knowing the response of photosynthesis to C_i under RuBP-limited conditions and the specificity of Rubisco, it is possible to estimate g_m . This method is valid only when J is constant. We have added the use of Chl fluorescence to the method described by Bongi and Loreto (1) as a rigorous method for estimating when J is constant. We shall call this the constant J method.

Another method, proposed by Di Marco *et al.* (5), relies on Chl fluorescence quenching analysis to estimate J. From the rate of electron transport and photosynthetic CO_2 assimilation, the rate of photorespiration can be calculated. From the rate of photorespiration and the specificity of Rubisco, C_c can be calculated. We shall call this method the variable J method. These two modeling methods require only a gas-exchange system and Chl fluorescence analysis.

In this report, we develop the theory behind these two methods and determine the sensitivity of the analyses to errors in the estimation of critical parameters such as the rate of R_d occurring during photosynthesis and the specificity of Rubisco for CO_2 . In the accompanying report, these two methods are compared with the isotopic method and used to determine g_m in a number of plant species (19).

THEORY

The drop in CO_2 partial pressure as CO_2 diffuses from the atmosphere to the chloroplast stroma is inversely proportional to the conductance of each step. Thus

$$A = (C_a - C_i) \cdot g_s / P = (C_i - C_c) \cdot g_m / P, \quad (1)$$

where P is the atmospheric pressure.

The units of conductance depend upon how the driving force is expressed (4). Current units for stomatal conductance are usually defined with the mole fraction (mixing ratio) implicit. Because mole fraction is unitless, the units for conductance appear the same as those for photosynthesis (4).

However, as CO_2 diffuses into the mesophyll, it must enter the liquid phase of the mesophyll cell. The amount of gas that dissolves in a liquid depends upon the partial pressure of the gas above the liquid according to Henry's law. If the dissolution of CO_2 into the liquid phase or diffusion through the liquid phase are the predominant components of g_m , then it is most appropriate to use partial pressure for the driving force, which leads to conductance units of $\text{mol m}^{-2} \text{s}^{-1} \text{bar}^{-1}$. We will follow the precedent laid down by von Caemmerer and Evans (30) and express g_m in these units. This conductance is directly comparable to g_s when the atmospheric pressure is 1 bar.

Current models of C_3 leaf photosynthesis assume that carboxylation of RuBP by Rubisco is limited by one of three factors (7, 14, 23, 24). These are (a) the activity of Rubisco, (b) the regeneration of RuBP, or (c) the release of phosphate during the metabolism of triose phosphate to either starch or sucrose. Over periods of several hours to several days photosynthesis will be limited by both CO_2 availability and light availability; it is only over short measurement intervals that photosynthesis can be considered to be limited predominantly by one or another factor (25).

When Rubisco activity limits photosynthesis, the following equation describes A:

$$A = \frac{V_{\text{cmax}} \cdot C_c}{C_c + K_C \cdot (1 + O/K_0)} \cdot \left(1 - \frac{\Gamma^*}{C_c}\right) - R_d, \quad (2)$$

where V_{cmax} is the V_{max} of Rubisco for carboxylation, K_C is the K_m of Rubisco for CO_2 , O is the partial pressure of O_2 , and K_0 is the K_i of Rubisco for O_2 . For our purposes, K_C , K_0 , and Γ^* are assumed constant at 25°C with values at 200 mbar O_2 of $K_C = 274 \mu\text{bar}$, $K_0 = 420 \text{ mbar}$, and $\Gamma^* = 43.08 \mu\text{bar}$. Substituting $C_i - A/g_m$ for C_c , Equation 2 becomes

$$A = \frac{V_{\text{cmax}} \cdot (C_i - A/g_m)}{(C_i - A/g_m) + K_C \cdot (1 + O/K_0)} \cdot \left(1 - \frac{\Gamma^*}{(C_i - A/g_m)}\right) - R_d. \quad (3)$$

When RuBP regeneration limits photosynthesis

$$A = J \cdot \frac{(C_i - A/g_m) - \Gamma^*}{4 \cdot ((C_i - A/g_m) + 2\Gamma^*)} - R_d, \quad (4)$$

the 4 arises by assuming 4 electrons per carboxylation or oxygenation (11). The rate of electron transport can be estimated from PFD assuming the empirical relationship

$$J = \frac{0.24 \text{ PFD}}{(1 + 0.24^2 \cdot \text{PFD}^2 / J_{\text{max}}^2)^{0.5}}, \quad (5)$$

where J_{max} is a theoretical maximum rate of J (13).

Equation 4 can be rearranged to

$$J = (A + R_d) \cdot \frac{4 \cdot ((C_i - A/g_m) + 2\Gamma^*)}{(C_i - A/g_m) - \Gamma^*}. \quad (6)$$

This equation applies to photosynthesis regardless of what assumptions are made about what limits photosynthesis and so can be used when electron transport is limiting (light is saturating) and when it is not.

The first method for estimating g_m from gas-exchange

analysis assumes that J is constant with changes in $p\text{CO}_2$. To estimate g_m , a value of g_m is assumed and used in Equation 6. This is done for three or more points of a CO_2 -response curve of A in which the fluorescence data indicated that J was constant. The variance $[\sum_{i=1}^n (J_a - J_i)^2 / (n - 1)]$, where J_a is the average value of J and J_i is the value for J for each C_i is then calculated. The value of g_m that gives the minimum variance is the best estimate of g_m by this method. The constant J method has the advantage that it can be based on a number of measurements of gas exchange, reducing the effect of error in individual measurements.

The constant J method is only valid when J is constant with changes in $p\text{CO}_2$. The rate of electron transport is highly regulated, falling when either Rubisco or phosphate release limits A , and the precise range of $p\text{CO}_2$ over which this method is valid is not obvious from CO_2 -response curves of photosynthetic CO_2 assimilation (26). To avoid ambiguities, we propose to use Chl fluorescence analysis to determine that range of $p\text{CO}_2$ over which J is constant. Although the exact relationship between J and Chl fluorescence quenching is uncertain, all methods agree that if there is no change in PFD and the various quenching parameters, then J also remains constant. If less than saturating PFD is used, it is easy to obtain a wide range of $p\text{CO}_2$ over which J is constant.

The variable J method is also based on Equation 6, but instead of assuming that J remains constant, J is estimated from Chl fluorescence parameters. Rearranging Equation 6 allows g_m to be calculated directly

$$g_m = \frac{A}{C_i - \frac{\Gamma^* \cdot [J + 8 \cdot (A + R_d)]}{J - 4 \cdot (A + R_d)}} \quad (7)$$

Advantages of the variable J method are that estimates can be made at specific CO_2 partial pressures and J need not be constant. Disadvantages are that errors in gas-exchange and fluorescence measurements affect the estimates of g_m and that uncertainties about the relationship between fluorescence parameters and J make estimates of g_m by the variable J method less robust.

METHODS

Chl Fluorescence

Chl fluorescence yield was measured with a PAM fluorometer from Heinz Walz (Effeltrich, Germany). The end of the polyfurcated fiber optic light guide was held at 45° to the leaf surface. For the constant J method, we identified the range of $p\text{CO}_2$ over which fluorescence yield did not change with $p\text{CO}_2$. For the variable J method, we determined J as described by Cornic and Briantais (3). From Genty *et al.* (12)

$$J = k\Delta F/F_m, \quad (8)$$

where k is some proportionality constant that depends upon the PFD and could vary from leaf to leaf and between different measuring systems, F_m is fluorescence yield during a saturating pulse of light, and ΔF is the difference between F_m and F_s , the steady-state fluorescence yield. The value for k was determined by measuring the rate of photosynthesis and fluorescence yield under nonphotorespiratory conditions (>1000

$\mu\text{bar CO}_2$ or <20 mbar O_2 or both). Because the PFD was maintained constant, changes in $\Delta F/F_m$ were related to J as described by Equation 8 and J was determined for every measurement of $\Delta F/F_m$.

Gas Exchange

Measurements of gas exchange were made as described in the accompanying paper (19).

RESULTS

Constant J Method

A theoretical response of photosynthesis was generated to help determine the effects of g_m on gas-exchange characteristics of leaves. To this ideal CO_2 response we introduced a finite g_m (Fig. 1). As g_m was reduced from infinity (where $C_c = C_i$), the rate of photosynthesis at a given C_i declined. The family of curves in Figure 1 was analyzed by determining the variance in J as the estimate of g_m was changed. The results are shown in Figure 2. The variance reached a minimum (zero in this case of ideal data) at the value of g_m used to generate the curve, as expected. We found that the variance was well behaved with a single minimum. The minimum was sharpest at the lowest value for g_m . At the highest value of g_m , the minimum in variance occurred over such a large range that it is of little use in estimating g_m .

The constant J method was fairly insensitive to errors in R_d but substantially more sensitive to errors in Γ^* (Fig. 3). In both cases, the error was greater when g_m was high than when it was low. For $g_m < 0.4 \text{ mol m}^{-2} \text{ s}^{-1} \text{ bar}^{-1}$, the error introduced by a $\pm 10\%$ error in the estimation of R_d was less than 3%. The error in the estimate of g_m was more strongly affected by errors in Γ^* when $g_m = 0.4 \text{ mol m}^{-2} \text{ s}^{-1} \text{ bar}^{-1}$, a 10% underestimate of Γ^* resulted in a 32% underestimate of g_m , and a 10% overestimate resulted in a 92% overestimate of g_m .

Typical experimental data obtained using a leaf of *Quercus rubra* is shown in Figure 4. Although A increased over the

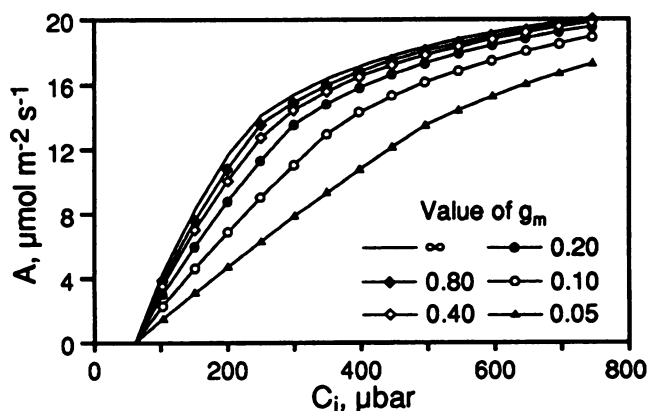


Figure 1. An ideal data set generated using the equations in the "Theory" section. Irradiance was assumed to be $750 \mu\text{mol m}^{-2} \text{ s}^{-1}$ and temperature was 25°C . Different responses of A to C_i were generated by imposing different values of g_m as indicated on the figure.

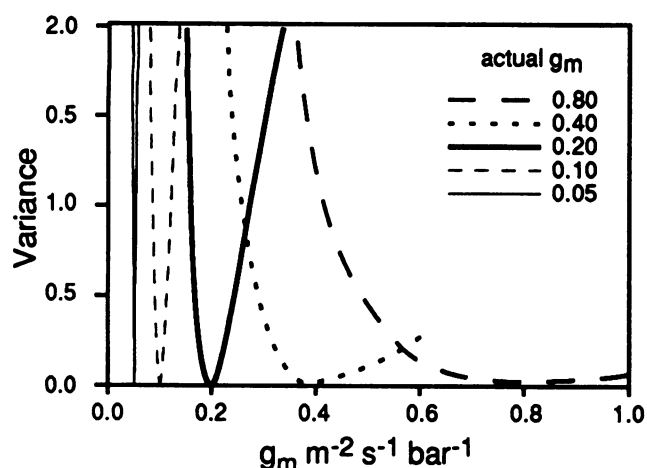


Figure 2. Variance as a function of g_m as determined by the constant J method using the data of Figure 1.

whole range of $p\text{CO}_2$, fluorescence reached a plateau at 350 μbar (Fig. 4A). The best fit of the model of photosynthesis when g_m is assumed infinite ($C_c = C_i$) (Fig. 4B) underestimated the CO_2 sensitivity of photosynthesis over that region where fluorescence indicated that J was constant. Next, data in that region where RuBP regeneration was constant were used to find the variance in estimates of J assuming various values for g_m (Fig. 4C). The minimum variance occurred at $g_m = 0.083 \text{ mol m}^{-2} \text{ s}^{-1} \text{ bar}^{-1}$. In this measured data set, the variance did not reach zero as it did in the ideal data sets, but a single, distinct minimum was observed. The model of photosynthesis was fit to the data again, this time assuming a g_m of $0.083 \text{ mol m}^{-2} \text{ s}^{-1} \text{ bar}^{-1}$. With this assumption, the model predictions for the CO_2 response of photosynthesis were closer to the measured values (Fig. 4D) than when g_m was assumed to be infinite (Fig. 4B). The introduction of g_m required much more Rubisco activity and a higher J to account for the rates of photosynthesis.

Variable J Method

The constant J method worked well over a large range of CO_2 , but to resolve the effect of CO_2 on g_m required the variable J method. The effect of CO_2 on g_m was determined using Equation 7 and estimating J from Chl fluorescence and PFD. In addition to the uncertainties in R_d and Γ^* , this method can be in error if the estimate of J is in error. The errors in the estimate of g_m introduced into an ideal data set by varying the values for J , R_d , and Γ^* by up to 10% are summarized in Figure 5. For this analysis, C_i was set to 250 μbar . As with the constant J method, the estimate of g_m using the variable J method was increasingly sensitive to errors as the value of g_m was increased. In addition, the estimate of g_m was much more sensitive to errors in J and Γ^* than in R_d . For $g_m = 0.2 \text{ mol m}^{-2} \text{ s}^{-1} \text{ bar}^{-1}$, a 10% overestimate in R_d gave a 5% overestimate of g_m , for Γ^* the error was 53%, and for J a 31% underestimate. A 10% overestimate of R_d led to a 4% underestimate of g_m , for Γ^* a 26% underestimate, and for J a 233% overestimate (Fig. 5).

In addition, the sensitivity of the estimates depended upon

C_i . The error in the estimate of g_m introduced by a $\pm 5\%$ error in Γ^* or R_d and a $\pm 2\%$ error in J is shown as a function of C_i in Figure 6. In all cases, the sensitivity to errors was relatively low between 100 and 300 μbar C_i , but outside this range the sensitivity was so great that the results could become unreliable. We investigated several methods to test the sensitivity of the data to errors (data not shown). In the end, we settled on a relatively simple test; any set of data that satisfied our criterion was accepted and any set that fell outside the bounds we set was ignored. The method we developed is based on the relationship between C_c and $A + R_d$. Assuming Γ^* is fixed, there is a family of curves representing different values of J (Fig. 7). We found that if the slope of the curve was too great, the sensitivity of g_m to small errors was too great. Likewise, if the slope was too low, the data were often unbelievable. The acceptable range was described by the slope of C_c versus $(A + R_d)$. Because

$$C_c = \Gamma^* \cdot [J + 8 \cdot (A + R_d)] / [J - 4 \cdot (A + R_d)], \quad (9)$$

then

$$dC_c/dA = 12 \cdot \Gamma^* \cdot J / [J - 4 \cdot (A + R_d)]^2. \quad (10)$$

We determined that data in the range of $10 < dC_c/dA < 50$ were reliable. Any data set that fit this criterion (unshaded region in Fig. 7) was accepted; data points outside this range

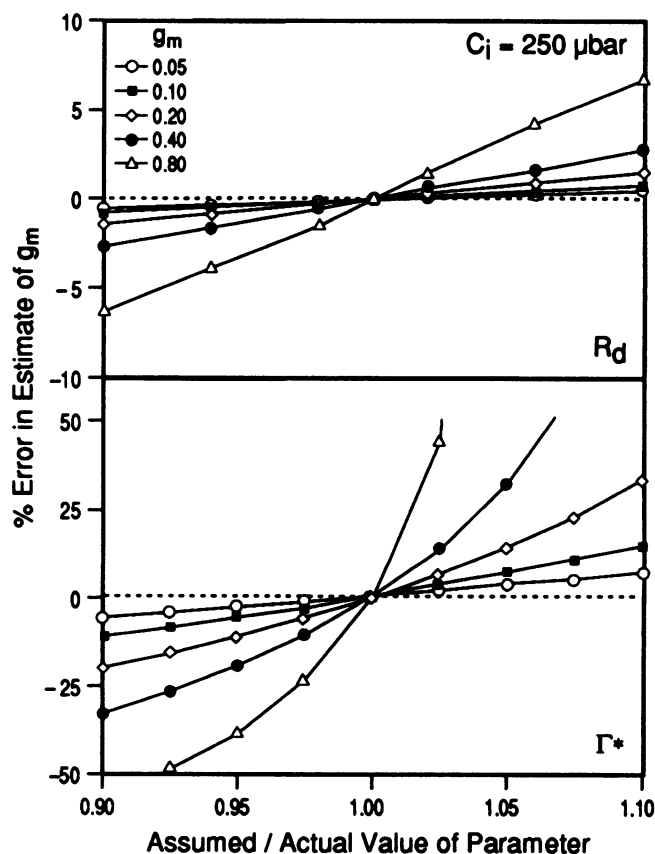


Figure 3. Errors in the estimate of g_m caused by using up to $\pm 10\%$ of the correct value for R_d or Γ^* . This error analysis applies to the data in Figure 2.

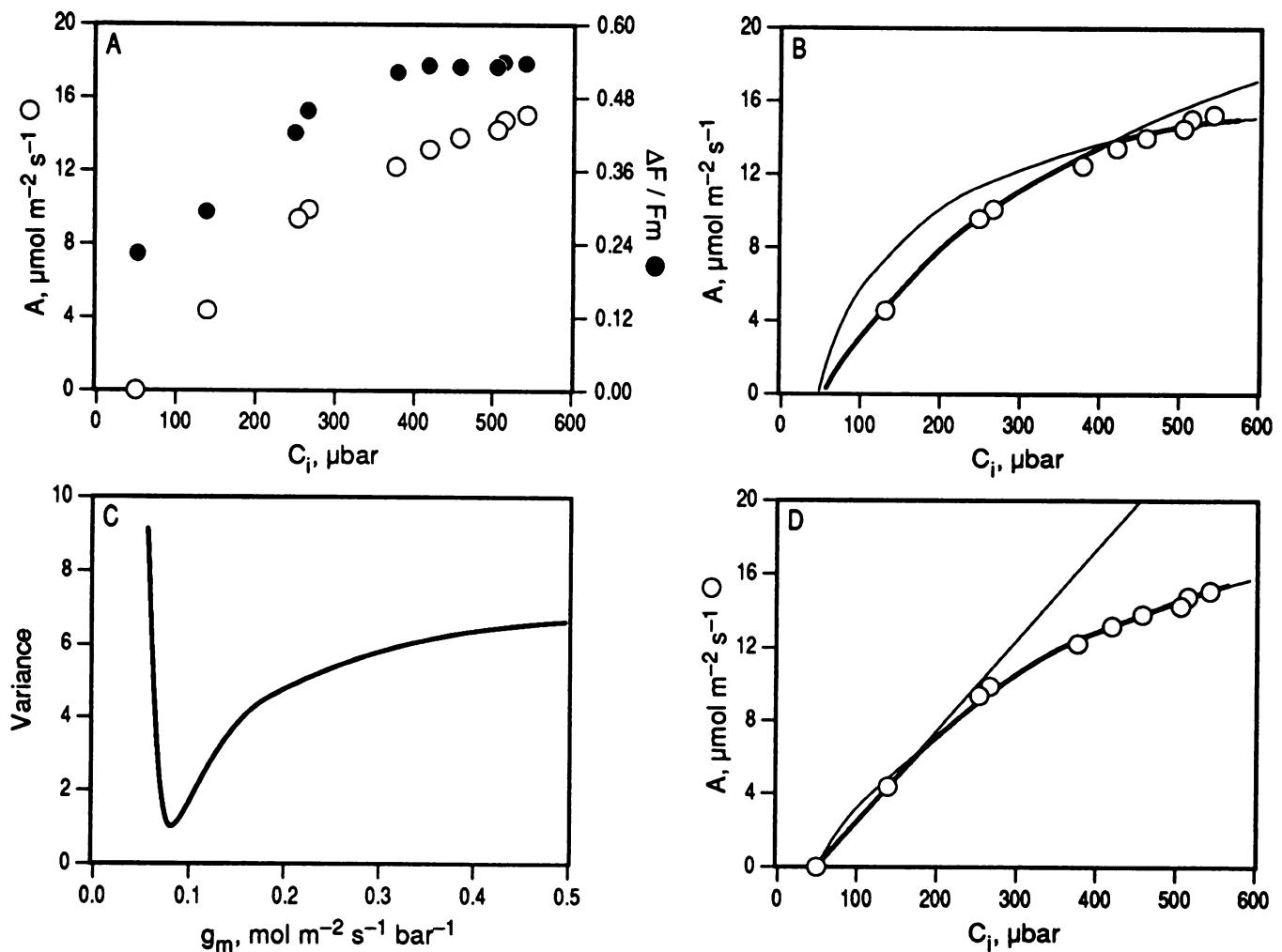


Figure 4. Experimental data from a leaf of *Q. rubra*. In A, photosynthetic CO₂ assimilation and $\Delta F/F_m$ are shown as functions of C_i . The best fit of the model of photosynthesis with infinite g_m developed in the "Theory" section is shown in B. The light lines represent the extensions of Rubisco or RuBP regeneration-limited photosynthesis in regions where photosynthesis was limited by another process. From this curve fitting, maximum Rubisco activity was $32 \mu\text{mol m}^{-2} \text{s}^{-1}$ and J was $77 \mu\text{mol m}^{-2} \text{s}^{-1}$. The variance in J over the highest six points determined by the constant J method is shown in C. In D, the fit of the model assumes $g_m = 0.083 \text{ mol m}^{-2} \text{s}^{-1} \text{bar}^{-1}$. In this case, the maximum Rubisco activity was $58 \mu\text{mol m}^{-2} \text{s}^{-1}$ and J was $90 \mu\text{mol m}^{-2} \text{s}^{-1}$.

(shaded regions in Fig. 7) were judged unacceptable. Many of these g_m values were negative or unbelievably high, although other points outside the acceptable range fit the expected value.

The application of the variable J method to experimental data obtained with *Q. rubra* and *Eucalyptus globulus* is shown in Figure 8. In the case of *Q. rubra*, one measurement of g_m at low C_i was higher than the rest; in *E. globulus*, g_m appeared to be unaffected by C_i .

DISCUSSION

We have studied two similar techniques for determining g_m , both of which require a standard gas-exchange measurement apparatus and the capability of simultaneously measuring steady-state Chl fluorescence but do not require a ratio mass spectrometer. In the constant J method, model parameters requiring estimation are R_d and Γ^* ; it is sufficient to

demonstrate that J is constant over a given range of C_i values. For the variable J method, it is also necessary to obtain quantitative estimates of J .

Not surprisingly, both techniques were quite sensitive to measurement errors, particularly when g_m was high. The value of g_m is inversely proportional to $C_i - C_c$ (Eq. 1). As $C_i - C_c$ decreases, any error in the estimate of C_c exerts an increasingly large effect on the estimate of g_m . It is apparent in Figure 1 that the difference between the curves is reduced as g_m increases, until the difference between $g_m = 0.4$ and $g_m = 0.8 \text{ mol m}^{-2} \text{s}^{-1} \text{bar}^{-1}$ is very slight. Using ideal data sets generated by the model, these slight differences can be resolved, but applying the technique to measured gas-exchange data becomes increasingly problematic for g_m above approximately $0.4 \text{ mol m}^{-2} \text{s}^{-1} \text{bar}^{-1}$.

Both techniques were far more sensitive to errors in the estimation of Γ^* than to errors in R_d (Figs. 3 and 5); however,

the value of Γ^* is more certain than that of R_d . The value of Γ^* may be determined either from *in vitro* Rubisco assays (15, 16, 31, 32) or from careful analysis of measured leaf gas exchange (2). Regardless of the technique used, estimates of Γ^* have been remarkably conservative. On the other hand, both the interpretation and estimation of R_d remain problematic.

The variable J method was more sensitive to errors in R_d than the constant J method (Figs. 3 and 5) because the constant J method depends upon the response of $A + R_d$ to

pCO₂ and the variable J method depends upon the absolute value of $A + R_d$. The constant J method requires only that J remain constant over a range of C_i values, whereas the variable J method is quite sensitive to errors in the estimates of J determined from Chl fluorescence. The fluorescence technique is relatively new and the underlying framework for this estimation could change in the future. Furthermore, employing the variable J method requires that transport of electrons to noncarboxylation reactions, such as nitrite reduction, remain a constant proportion of J.

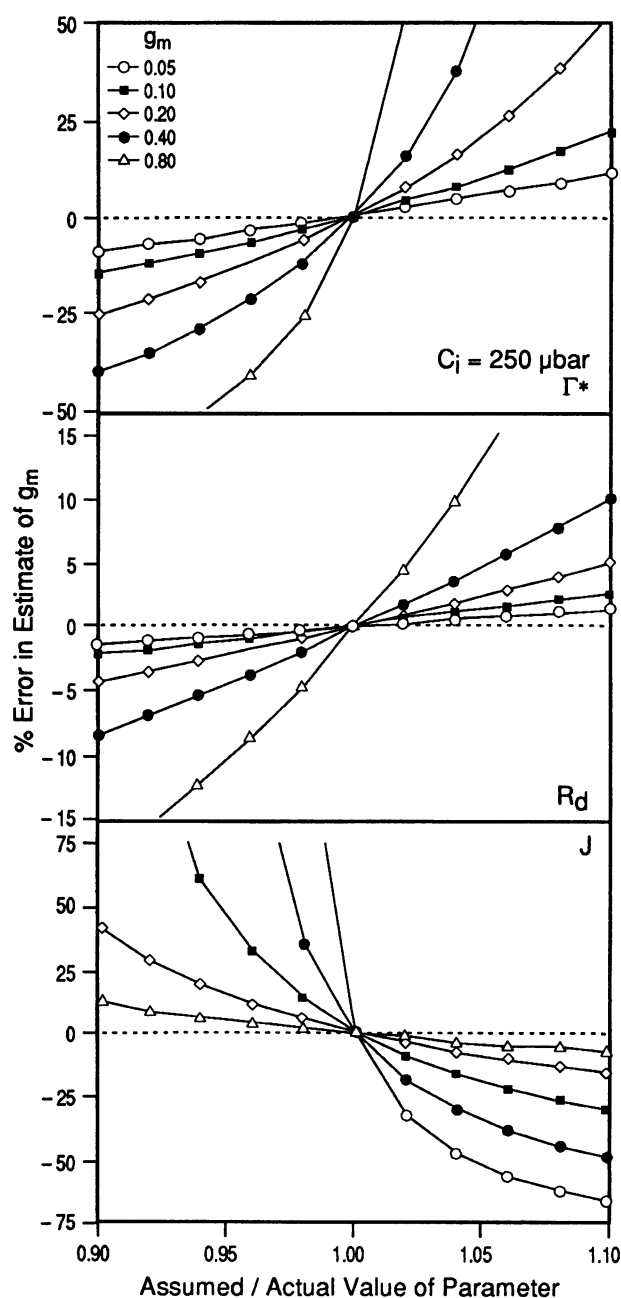


Figure 5. Errors in the estimate of g_m induced by using $\pm 10\%$ of the correct value for Γ^* , R_d , and J using the variable J method for determining g_m .

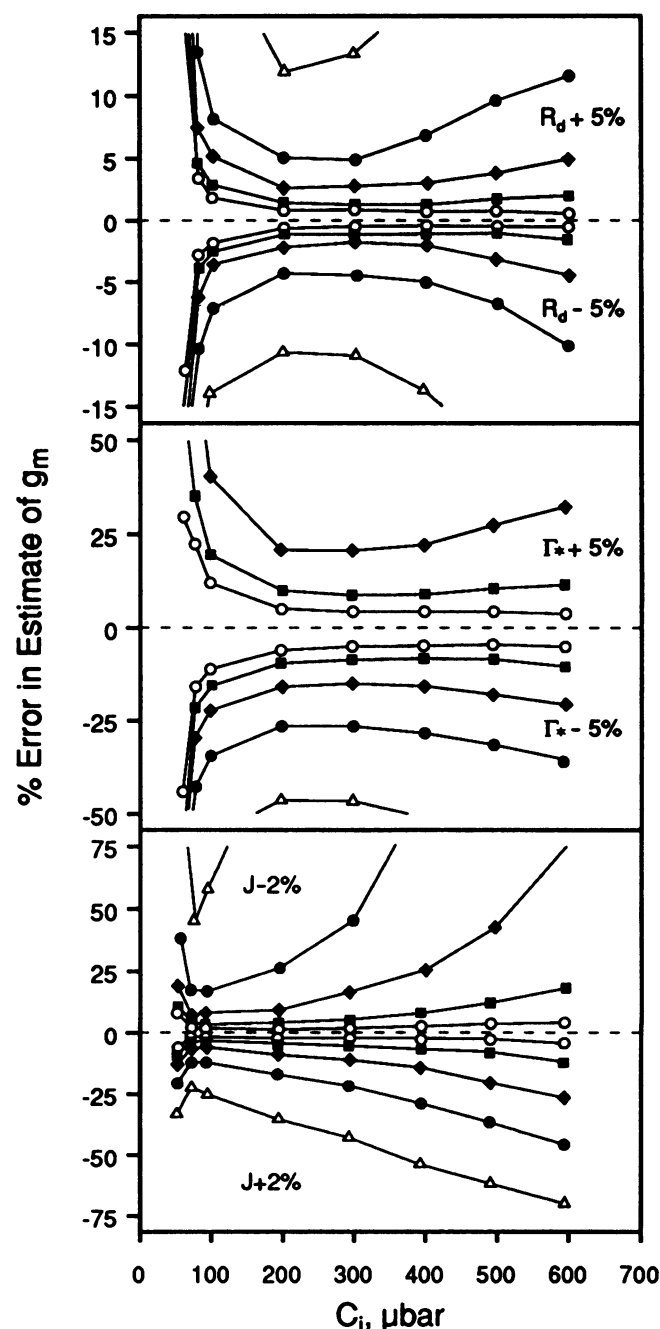


Figure 6. Errors in the variable J method caused by $\pm 5\%$ error in R_d and Γ^* or a $\pm 2\%$ error in J as functions of C_i .

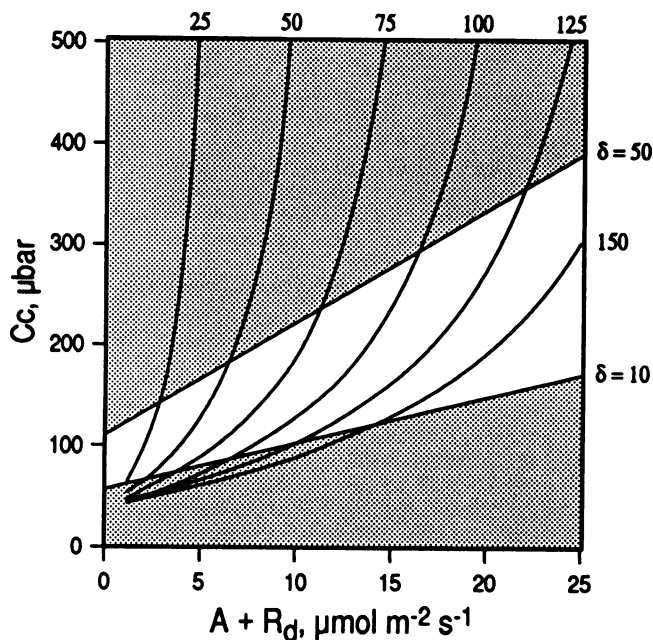


Figure 7. Plot of C_c versus $A + R_d$ assuming different values for J . The values used for J are identified along the top of the graph in $\mu\text{mol m}^{-2} \text{s}^{-1}$. The line showing where $dC_c/dA = 50$ ($\delta = 50$) and the line showing $\delta = 10$ are drawn. Only data lying between these two lines were used for analyses because the method became too sensitive to small errors in the data when data were in the shaded areas.

Given the potential errors in estimations made by the variable J method, we chose to call measurements in which dC_c/dA was less than 10 or more than 50 unreliable. However, the estimates of J by fluorescence appear empirically correct and Cornic and Briantais (3) have confirmed that the specificity of Rubisco in plant extracts is similar to that measured in intact leaves using fluorescence techniques. Thus, we feel that the relationship between fluorescence and J is well-enough known to justify its use in the way we describe here.

In Figure 8, there are six estimates of g_m for *Q. rubra* averaging $0.137 \pm 0.027 \text{ mol m}^{-2} \text{s}^{-1} \text{bar}^{-1}$, and six estimates for *E. globulus* averaging 0.115 ± 0.026 . Using the constant J method, we obtained a value of $0.083 \text{ mol m}^{-2} \text{s}^{-1} \text{bar}^{-1}$ for a different leaf of *Q. rubra*. These fall below the low end of values reported by von Caemmerer and Evans (30), which ranged from $0.15 \text{ mol m}^{-2} \text{s}^{-1} \text{bar}^{-1}$ for leaves with low rates of CO_2 assimilation to $0.52 \text{ mol m}^{-2} \text{s}^{-1} \text{bar}^{-1}$ for leaves with extremely high rates. Given the low photosynthesis rates in our study (Figs. 4 and 8), low values of g_m were expected and are consistent with the linear relationship between g_m and A found by von Caemmerer and Evans (30). von Caemmerer and Evans reported an average value of 0.7 for the ratio between C_c and C_i when $C_a = 350 \mu\text{bar}$. For *Q. rubra* and *E. globulus* we determined values of 0.72 and 0.63, respectively, using the variable J method, whereas the constant J method yielded 0.55 for *Q. rubra*.

We believe that the two methods developed here will prove useful for estimating g_m in many species. Because these methods are substantially easier than the isotopic method available until now, many more investigators may now be able to

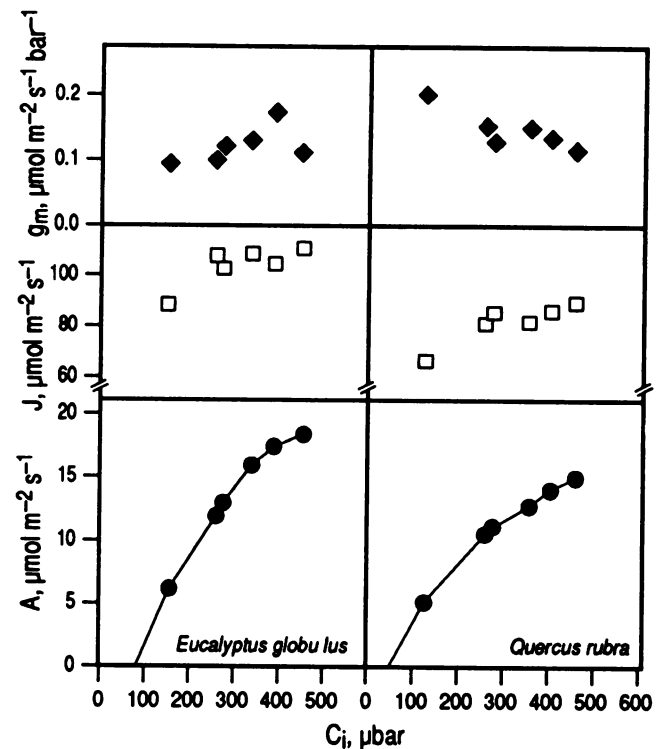


Figure 8. Plot of g_m , J , and A as functions of C_i . The calculation of J was made from Chl fluorescence and g_m was calculated by the variable J method. Data are shown for *E. globulus* and *Q. rubra*.

determine g_m . Each method has its advantages: the constant J method is somewhat less sensitive to errors, whereas the variable J method can be used to determine the effect of $p\text{CO}_2$ on g_m . In the accompanying paper (19), these two methods are compared with the isotopic method and all of the methods are used to determine g_m of a large number of species and to obtain more data on the effect of CO_2 on g_m .

ACKNOWLEDGMENTS

We thank Drs. Graham Farquhar, David Parkhurst, and Jim Syvertson for helpful comments on earlier versions of the manuscript.

LITERATURE CITED

- Bongi G, Loreto F (1989) Gas-exchange properties of salt-stressed olive (*Olea europaea* L.) leaves. *Plant Physiol* 90: 1408–1416
- Brooks A, Farquhar GD (1985) Effects of temperature on the O_2/CO_2 specificity of ribulose-1,5-bisphosphate carboxylase/oxygenase and the rate of respiration in the light. Estimates from gas exchange measurements on spinach. *Planta* 165: 397–406
- Cornic G, Briantais J-M (1991) Partitioning of photosynthetic electron flow between CO_2 and O_2 reduction in a C_3 leaf (*Phaseolus vulgaris* L.) at different CO_2 concentrations and during drought stress. *Planta* 183: 178–184
- Cowan IR (1977) Stomatal behavior and environment. *Adv Bot Res* 4: 117–228
- Di Marco G, Manes F, Tricoli D, Vitale E (1990) Fluorescence parameters measured concurrently with net photosynthesis to investigate chloroplastic CO_2 concentration in leaves of *Quercus ilex* L. *J Plant Physiol* 136: 538–543
- Evans JR, Sharkey TD, Berry JA, Farquhar GD (1986) Carbon

- isotope discrimination measured concurrently with gas exchange to investigate CO₂ diffusion in leaves of higher plants. *Aust J Plant Physiol* **13**: 281–292
7. **Farquhar GD** (1989) Models of integrated photosynthesis of cells and leaves. *Philos Trans R Soc Lond B Biol Sci* **323**: 357–367
 8. **Farquhar GD, O'Leary MH, Berry JA** (1982) On the relationship between carbon isotope discrimination and the intercellular carbon dioxide concentration in leaves. *Aust J Plant Physiol* **9**: 121–137
 9. **Farquhar GD, Sharkey TD** (1982) Stomatal conductance and photosynthesis. *Annu Rev Plant Physiol* **33**: 317–345
 10. **Farquhar GD, von Caemmerer S** (1982) Modelling of photosynthetic response to environmental conditions. In OL Lange, PS Nobel, CB Osmond, H Ziegler, eds, *Encyclopedia of Plant Physiology NS Vol 12B. Physiological Plant Ecology II: Water Relations and Carbon Assimilation*. Springer-Verlag, Berlin, pp 549–587
 11. **Farquhar GD, von Caemmerer S, Berry JA** (1980) A biochemical model of photosynthetic CO₂ assimilation in leaves of C₃ species. *Planta* **149**: 78–90
 12. **Genty B, Briantais J-M, Baker NR** (1989) The relationship between the quantum yield of photosynthetic electron transport and quenching of chlorophyll fluorescence. *Biochim Biophys Acta* **990**: 87–92
 13. **Harley PC, Thomas RB, Reynolds JF, Strain BR** (1992) Modeling photosynthesis of cotton growth in elevated CO₂. *Plant Cell Environ* (in press)
 14. **Harley PC, Sharkey TD** (1991) An improved model of C₃ photosynthesis at high CO₂: reversed O₂ sensitivity explained by lack of glycerate reentry into the chloroplast. *Photosynth Res* **28**: 169–179
 15. **Jordan DB, Ogren WL** (1981) A sensitive assay procedure for simultaneous determination of ribulose-1,5-bisphosphate carboxylase and oxygenase activities. *Plant Physiol* **67**: 237–245
 16. **Jordan DB, Ogren WL** (1984) The CO₂/O₂ specificity of ribulose 1,5-bisphosphate carboxylase/oxygenase. Dependence on ribulose bisphosphate concentration, pH and temperature. *Planta* **161**: 308–313
 17. **Laisk A** (1977) Kinetics of Photosynthesis and Photorespiration of C₃ Plants (in Russian). Nauka, Moscow
 18. **Lloyd J, Syvertson J** (1991) Mesophyll wall conductance and the partial pressure of CO₂ at chloroplasts of citrus and peach leaves (abstract No. 91). *Plant Physiol* **96**: 5–17
 19. **Loreto F, Harley PC, Di Marco G, Sharkey TD** (1992) Estimation of the mesophyll conductance to CO₂ flux by three different methods. *Plant Physiol* **98**: 1437–1443
 20. **Mott KA, O'Leary JW** (1984) Stomatal behavior and CO₂ exchange characteristics in amphistomatous leaves. *Plant Physiol* **74**: 47–51
 21. **Nobel PS** (1991) *Physicochemical and Environmental Plant Physiology*. Academic Press, San Diego
 22. **Parkhurst DF, Mott KA** (1990) Intercellular diffusion limits to CO₂ uptake in leaves. *Studies in air and helox*. *Plant Physiol* **94**: 1024–1032
 23. **Sage RF** (1990) A model describing the regulation of ribulose-1,5-bisphosphate carboxylase, electron transport, and triose phosphate use in response to light intensity and CO₂ in C₃ plants. *Plant Physiol* **94**: 1728–1734
 24. **Sharkey TD** (1985) Photosynthesis in intact leaves of C₃ plants: physics, physiology and rate limitations. *Bot Rev* **51**: 53–105
 25. **Sharkey TD** (1989) Evaluating the role of rubisco regulation in C₃ photosynthesis. *Philos Trans R Soc Lond B Biol Sci* **323**: 435–448
 26. **Sharkey TD, Berry JA, Sage RF** (1988) Regulation of photosynthetic electron-transport as determined by room-temperature chlorophyll *a* fluorescence in *Phaseolus vulgaris* L. *Planta* **176**: 415–424
 27. **Sharkey TD, Imai K, Farquhar GD, Cowan IR** (1982) A direct conformation of the standard method of estimating intercellular partial pressure of CO₂. *Plant Physiol* **69**: 657–659
 28. **Terashima I, Wong S-C, Osmond CB, Farquhar GD** (1988) Characterisation of non-uniform photosynthesis induced by abscisic acid in leaves having different mesophyll anatomies. *Plant Cell Environ* **29**: 385–394
 29. **Troughton JH, Slatyer RO** (1969) Plant water status, leaf temperature, and the calculated mesophyll resistance to carbon dioxide of cotton leaves. *Aust J Biol Sci* **22**: 815–827
 30. **von Caemmerer S, Evans JR** (1991) Determination of the CO₂ pressure in chloroplasts from leaves of several C₃ plants. *Aust J Plant Physiol* **18**: 287–305
 31. **Yeoh H-H, Badger MR, Watson L** (1980) Variations in K_m(CO₂) of RuBPCase among grasses. *Plant Physiol* **66**: 1110–1112
 32. **Yeoh H-H, Badger MR, Watson L** (1981) Variations in kinetic properties of RuBPCase among plants. *Plant Physiol* **67**: 1151–1155